AIP ADVANCES 7, 025302 (2017)

Unified model for the electromechanical coupling factor of orthorhombic piezoelectric rectangular bar with arbitrary aspect ratio

R. Rouffaud,[1,2,a] F. Levassort,[2] and A.-C. Hladky-Hennion[1]
[1]*Univ. Lille, CNRS, Centrale Lille, ISEN, Univ. Valenciennes, UMR 8520 - IEMN, F-59000 Lille, France*
[2]*François-Rabelais University, GREMAN UMR 7347 CNRS, 37071 Tours, France*

(Received 3 December 2016; accepted 30 January 2017; published online 13 February 2017)

Piezoelectric Single Crystals (PSC) are increasingly used in the manufacture of ultrasonic transducers and in particular for linear arrays or single element transducers. Among these PSCs, according to their microstructure and poled direction, some exhibit a mm2 symmetry. The analytical expression of the electromechanical coupling coefficient for a vibration mode along the poling direction for piezoelectric rectangular bar resonator is established. It is based on the mode coupling theory and fundamental energy ratio definition of electromechanical coupling coefficients. This unified formula for mm2 symmetry class material is obtained as a function of an aspect ratio (G) where the two extreme cases correspond to a thin plate (with a vibration mode characterized by the thickness coupling factor, k_t) and a thin bar (characterized by k'_{33}). To optimize the k'_{33} value related to the thin bar design, a rotation of the crystallogaphic axis in the plane orthogonal to the poling direction is done to choose the highest value for PIN-PMN-PT single crystal. Finally, finite element calculations are performed to deduce resonance frequencies and coupling coefficients in a large range of G value to confirm developed analytical relations. © *2017 Author(s). All article content, except where otherwise noted, is licensed under a Creative Commons Attribution (CC BY) license (http://creativecommons.org/licenses/by/4.0/).* [http://dx.doi.org/10.1063/1.4976298]

I. INTRODUCTION

With the recent developments for single crystal growth methods,[1] scientists investigate new material compositions to improve piezoelectric properties. In particular, the relaxor-PT single crystals are already used in various transducer applications[2] for their high coupling capability. Lead-free single crystals are also extensively studied in order to satisfy new international restrictions.[3] Some of these crystals can exhibit orthorhombic structures like the well-known PIN-PMN-PT[4] or the promising lead-free $KNbO_3$,[5,6] that brings some difficulties in the optimization and the design of these piezoelectric materials for their integration in ultrasonic transducers. Indeed, in linear or phased arrays, piezoelectric elements shape is a rectangular slender bar with dimensions that depend on the expected transducer's characteristics (operating frequency, resolution, ...). This configuration was developed to reach an effective electromechanical coupling coefficient equal to k'_{33},[7] which is higher than the coupling coefficient for a thin plate, k_t. If the poling direction is assumed to be collinear to the spatial z–direction, the crystal orientation in the xy–plane makes the effective electromechanical coupling coefficient change contrary to a piezoceramic with a tetragonal or a transversaly isotropic structure. Moreover, the aspect ratio of the resonator's dimensions is the second factor that determines the effective coupling coefficient.

In some situations, such as high frequency transducers (>20MHz), it is very difficult for technical reasons to respect the aspect ratio recommended by the IEEE standard for piezoelectricity[8] to reach

[a]Corresponding author: remi.rouffaud@univ-tours.fr

 © Author(s) 2017

the k'_{33} value. Then, the effective coupling coefficient takes a different value that cannot be determined with accuracy because of an arbitrary aspect ratio.

In this paper, we propose a unified formula to calculate the electromechanical coupling coefficient for a rectangular slender bar. It is a generalization of the work performed by Kim *et al.*[9] to the case of orthorhombic materials that implies an additional study about the crystal orientation. The finite element calculation is also used to confirm the analytical results. In a first part, characteristic modes for the studied sample are chosen and the corresponding resonance frequencies are calculated. In the second part, analytical expression for the electromechanical coupling coefficient is established.

II. RESONANCE FREQUENCIES OF THE CHARACTERISTIC MODES

First, the resonance frequencies of the resonator are determined using an approach based on the mode coupling theory. The method gives accurate results in the case of elastic bodies[10] but can easily take into account piezoelectric coupling.[7,11] In this paper, a piezoelectric rectangular bar is supposed to be infinite in the y–direction, poled along its thickness (direction z) (Figure 1). Its width, along the x–direction, is denoted L and its thickness (or height) along the z–direction is H. Then, the aspect ratio G is chosen equal to H/L. When G is much smaller than 1, the resonator is a thin plate (Figure 1.a), whereas when G is much greater that 1, the resonator is an infinite slender bar (Figure 1.b). In this case, modes that are considered in the mode coupling theory are the modes along the z- and x-direction.[7] In the following they are differentiated respectively by the adjectives longitudinal and transversal.

In a first step, the resonance frequencies of the longitudinal mode are defined. The resonance frequency f_b for a thin plate is:[12]

$$f_b = \frac{1}{H}\sqrt{\frac{c_{33}^D}{\rho}}\frac{X_t}{\pi} \tag{1}$$

with X_t solution of $X_t - k_t^2 \tan(X_t) = 0$, c_{33}^D is the stiffness constant from the elastic tensor at constant electric displacement, ρ is the density and $k_t = e_{33}/\sqrt{c_{33}^D \epsilon_{33}^S}$ is the electromechanical coupling coefficient for the longitudinal thickness-extensional (L-TE) mode. The L-TE resonance frequency is independent of the width L and is inversely proportional to H. One can also define the resonance frequency f_d for a slender bar,[7] which is inversely proportional to H and where k'_{33} is the electromechanical coupling coefficient for this longitudinal width-extensional (L-WE) mode:

$$f_d = \frac{1}{H}\sqrt{\frac{\tilde{c}_{33}^D}{\rho}}\frac{\tilde{X}_s}{\pi} \tag{2}$$

with $\tilde{X}_s$ solution of $\tilde{X}_s - k'^2_{33} \tan(\tilde{X}_s) = 0$ and $\tilde{c}_{33}^D = c_{33}^D - \left(c_{13}^D\right)^2 / c_{11}^D$. Then, two transversal resonance frequencies are defined,[7] either for an infinite slender bar or for a thin plate. The first one, that is the transversal thickness-extensional (T-TE) mode, is:

$$f_a = \frac{1}{2L}\sqrt{\frac{c_{11}^E}{\rho}}. \tag{3}$$

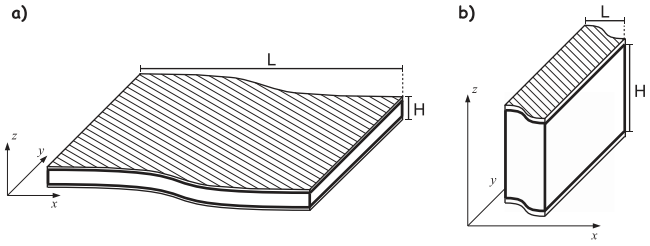


FIG. 1. Description of the geometry of the piezoelectric element ($G = H/L$): a) G is small ($G << 1$), the resonator is a thin plate and b) G is large ($G > 1$), the resonator is an infinite slender bar (hatching parts are the electrodes).

By introducing $G = H/L$ in Eq. 3, then f_a depends on G and is inversely proportional to H. In the same way, the other transversal resonance frequency f_c for the transversal width-extensional (T-WE) mode is defined as:[7]

$$f_c = \frac{1}{2L}\sqrt{\frac{\tilde{c}_{11}^E}{\rho}} \tag{4}$$

with $\tilde{c}_{11}^E = c_{11}^E\left(1 - {c_{13}^E}^2/\left(c_{11}^E c_{33}^E\right)\right)$ where c^E is the elastic tensor at constant electric field. One can notice that, for a fixed value of the thickness H, f_a and f_c linearly depend on the aspect ratio G, whereas f_b and f_d are constant whatever the value of G.

For the problem under study, the vibrating system is supposed to possess only two coupled degrees of freedom related to a longitudinal and a transversal mode. Therefore, the resonance frequencies can be analysed using the following equation:[7,11]

$$\left(f^2 - f_a^2\right)\left(f^2 - f_b^2\right) = \Gamma^2 f_a^2 f_b^2 \tag{5}$$

with the frequencies f_a, f_b defined above and the mode coupling factor Γ defined[7] by:

$$\Gamma = \sqrt{1 - \left(\frac{f_d}{f_b}\right)^2} = \sqrt{1 - \left(\frac{f_c}{f_a}\right)^2}. \tag{6}$$

On the one hand, Γ is a link between the two longitudinal frequencies f_b and f_d (L-TE and L-WE modes). On the other hand, Γ is the link between the two transversal frequencies f_a and f_c (T-TE and T-WE modes). In Eq. 6, the coupling factor Γ is supposed to be the same for the longitudinal and transversal modes. This hypothesis will be checked further for the material under interest. Eq. 5 supposes that only two modes interact. Solving Eq. 5 gives two solutions, named f_1 (the smaller root) and f_2 (the higher root):

$$f_{1,2} = \sqrt{\frac{f_a^2 + f_b^2 \pm \sqrt{\left(f_a^2 + f_b^2\right)^2 - 4 f_a^2 f_b^2\left(1 - \Gamma^2\right)}}{2}} \tag{7}$$

The analytical values of the f_a, f_b, f_c, f_d, f_1 and f_2 resonance frequencies (eqs. (1) to (4) and (7)) are first calculated for the PIN-PMN-PT single crystal,[4] which has an orthorhombic symmetry class. The corresponding properties are presented in Table I in standard coordinate system (material's crystallographic axes).

Because this material belongs to the mm2 point group, two orientations of the crystal in the *xy*–plane are considered. The first one is called 'standard', where the crystallographic axis in the direction 1 corresponds to the spatial vector $\vec{x}$ (Figure 2). The other one is called 90°–rotation and corresponds to a 90° rotation of the crystal around the *z*–axis. Fig. 3 presents the different analytical resonance frequencies multiplied by H as a function of the aspect ratio G. On Fig. 3, the L-TE and L-WE modes do not depend on G (horizontal lines for f_b and f_d) whereas the T-TE and T-WE modes are proportional to G (inclined lines for f_a and f_c). As also mathematically verified, Fig. 3 shows that for low values of G, f_1 follows an inclined line close to f_c, whereas f_2 is close to the horizontal line f_b. For large values of G, f_1 is close to the horizontal line f_d and f_2 follows an inclined line close to f_a. The link between the parallel lines of Fig. 3 is related to the mode coupling factor Γ (f_a and f_c on the one hand, f_b and f_d on the other hand).

TABLE I. Properties of the PIN-PMN-PT[4] single crystal. Elastic constants are expressed in 10^{-12} m^2/N, piezoelectric constants in 10^{-12} C/N, relative dielectric constants and density in kg/m^3.

s_{11}^E	s_{12}^E	s_{13}^E	s_{22}^E	s_{23}^E	s_{33}^E	s_{44}^E	s_{55}^E	s_{66}^E
9.2	-8.38	5.64	21.2	-14.4	16.8	78.1	31.6	15.5
ρ	d_{31}	d_{32}	d_{33}	d_{24}	d_{15}	$\epsilon_{11}^T/\epsilon_0$	$\epsilon_{22}^T/\epsilon_0$	$\epsilon_{33}^T/\epsilon_0$
8100	153	-346	350	4100	4550	8070	30000	1500

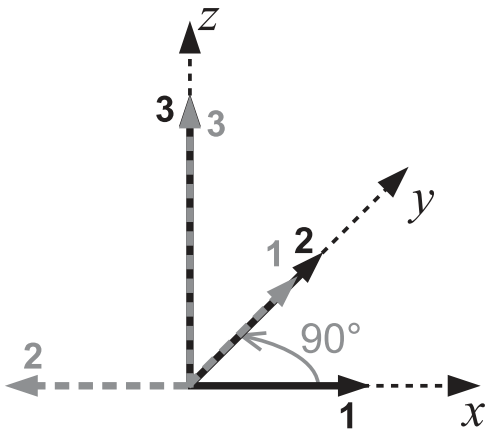


FIG. 2. Orientation of the crystallographic axes (123) according to the spatial frame (xyz) in the standard (in black) and the 90°−rotation (in gray) cases.

Table II presents the corresponding frequencies f_a, f_b, f_c, f_d mutilplied by H and calculated for $G = 0.1$. In the practical case of a thin plate resonator ($G = 0.1$) where the thickness is 215 μm, the thickness resonance frequency f_b is nearly equal to 10MHz. Moreover, the last two columns present the mode coupling factor Γ, calculated either with the longitudinal frequencies, or with the transversal frequencies. It shows that the mode coupling factor Γ is approximately the same, using one mode or the other. Therefore, the hypothesis considering the same mode coupling factor Γ for the longitudinal modes and the transversal modes is valid for the material under interest.

In order to check the values of the resonance frequencies, finite element calculations have been performed using the ATILA code.[13] The harmonic analysis gives the variations of the impedance

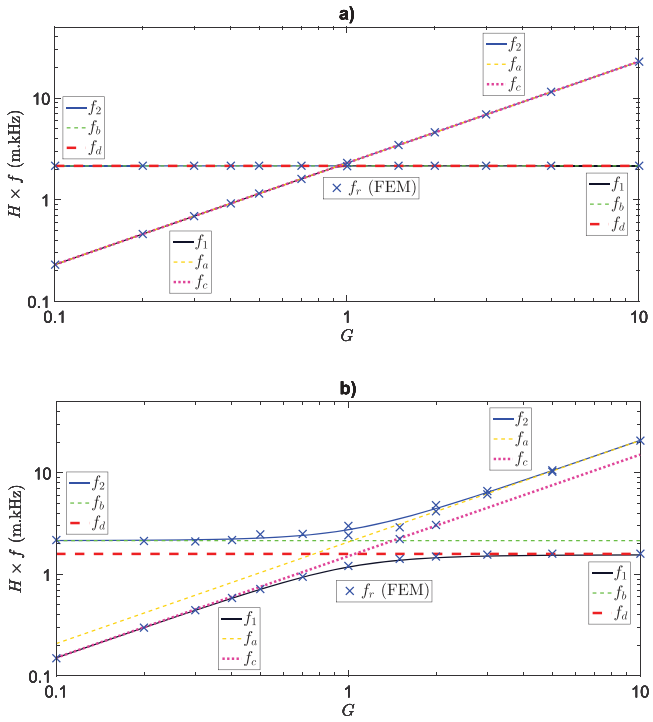


FIG. 3. Variations of the resonance frequencies multiplied by H as a function of the aspect ratio G, using the mode coupling theory for the PIN-PMN-PT single crystal in the (a) standard and (b) 90°−rotation cases. (Full lines : analytical results, dashed lines: extreme geometries, dots: FEM results). f_a, f_b, f_c, f_d, f_1 and f_2 are referred to Eqs. 1 to 4 and 7.

TABLE II. Frequencies multiplied by H of the longitudinal and transversal modes, defined by equations 1, 2, 3, and 4 for the PIN-PMN-PT single crystal. The transversal frequencies are calculated for the aspect ratio $G = 0.1$. The mode coupling factor Γ is calculated using Eq. 6: $\Gamma^{(1)} = \sqrt{1 - (f_c/f_a)^2}$ and $\Gamma^{(2)} = \sqrt{1 - (f_d/f_b)^2}$.

	Hf_a (m.Hz)	Hf_b (m.Hz)	Hf_c (m.Hz)	Hf_d (m.Hz)	$\Gamma^{(1)}$	$\Gamma^{(2)}$
Stand.	229	2147.5	229	2147	0.008	0.021
90°	208	2147.5	150.8	1589.5	0.688	0.672

versus frequency and allows the identification of the resonance and antiresonance frequencies. On the numerical impedance curves, some modes are easily identified, whereas some others are not purely related to a longitudinal mode or to a transversal mode. Numerical resonance frequencies are reproduced on Fig. 3 with dots, but only some of them are reproduced for a better clarity of the figure. For low values of the aspect ratio G, the lowest resonance frequency corresponds to the transversal mode, followed by many peaks with low electromechanical coupling factors. At higher frequency, one peak corresponds to the longitudinal mode but it is also mixed with other transversal modes. For large values of the aspect ratio G, the lowest resonance frequency corresponds to the longitudinal mode and is easily isolated. At higher frequency, many peaks appear in the impedance spectrum. In the intermediate region, when the aspect ratio G is around 1, several modes are observed. On Fig. 3, numerical resonance frequencies follow the f_1 and f_2 curves, validating the expression of the coupled modes (Eq. 7).

One can see that the mode coupling factor Γ is very low for the standard material: on the one hand, f_a and f_c are very close, on the other hand f_b and f_d are also very close. The longitudinal frequency does not depend on the aspect ratio G. In fact, an optimization of the material orientation can be performed in order to maximize the electromechanical coupling factor. Fig. 4.a presents the polar variations of the electromechanical coupling factors k_t and k'_{33} as a function of the material orientation in the (xy)–plane. k_t is constant (50%) for any orientation in the (xy)–plane whereas k'_{33} depends on the orientation in the (xy)–plane: it is around 50% for an angle equal to 0° and 68% at 90°. Fig. 4.b presents the polar variations of the f_b and f_d frequencies multiplied by H as a function of the orientation of the material in the (xy)–plane. One can notice that f_b is constant for any orientation in the (xy)–plane. The link between these two curves is clear: when the two electromechanical coupling factors k_t and k'_{33} are close, then the two frequencies f_b and f_d are close (see Eq. 1 and 2) and the mode coupling factor Γ is small. Reversely, as the difference between the two electromechanical coupling factors k_t and k'_{33} is higher, then the frequencies f_b and f_d are different and the mode coupling factor Γ is large. Therefore, Fig. 4 can be useful in order to determine which material orientation gives the highest difference between k_t and k'_{33}.

To conclude, this rotation in the xy–plane allows to examine the behavior of the two longitudinal modes (L-TE and L-WE) as a function of the crystal orientation, in order to maximise the coupling factor, that is essential for further applications using an orthorhombic material.

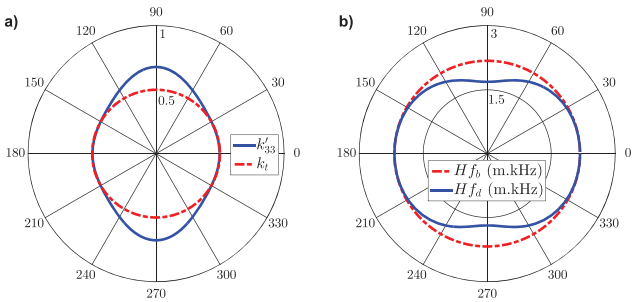


FIG. 4. Polar variations of (a) the electromechanical coupling factors k_t (dashed lines, red) and k'_{33} (solid lines, blue) and, (b) the $H \times f_b$ (dashed lines, red) and $H \times f_d$ (solid lines, blue) frequencies as a function of the orientation of the crystallographic axes in the (xy)-plane.

III. ELECTROMECHANICAL COUPLING COEFFICIENT

In order to calculate the electromechanical coupling coefficient of the resonator, the piezoelectric constitutive relations are written. They are very similar to the set of equations from the work of Kim et *al.*,[9,14] except that they are written for a mm2 symmetry class material. They can be simplified considering a 6mm or a 4mm symmetry class material reducing the number of independent constants. Due to the geometry of the resonator, the electric field and the electric displacement only exist in the z-direction ($E_3 \neq 0$ and $D_3 \neq 0$). Thus, the relations are:

$$S_1 = s_{11}^E T_1 + s_{12}^E T_2 + s_{13}^E T_3 + d_{31} E_3 \tag{8.a}$$

$$S_2 = s_{12}^E T_1 + s_{22}^E T_2 + s_{23}^E T_3 + d_{32} E_3 \qquad (=0) \tag{8.b}$$

$$S_3 = s_{13}^E T_1 + s_{23}^E T_2 + s_{33}^E T_3 + d_{33} E_3 \tag{8.c}$$

$$D_3 = d_{31} T_1 + d_{32} T_2 + d_{33} T_3 + \epsilon_{33}^T E_3 \tag{8.d}$$

The internal energy is:

$$U = \frac{1}{2}\left(S_1 T_1 + S_2 T_2 + S_3 T_3\right) + \frac{1}{2}\left(D_3 E_3\right) \tag{9}$$

In Eq. 9, the internal energy will be split further into three parts U_e, U_d and U_c that are respectively the elastic, dielectric and coupling energies. Then, the electromechanical coupling factor k is defined as:[7]

$$k = \frac{U_c}{\sqrt{U_e U_d}} \tag{10}$$

In order to determine each term of the internal energy, the procedure is the following: using Eq. 8.b, T_2 is expressed as a function of T_1, T_3 and E_3. It is then inserted into equations 8.a, 8.c and 8.d thus S_1, S_3 and D_3 do not depend on T_2:

$$S_1 = \left(s_{11}^E - \frac{{s_{12}^E}^2}{s_{22}^E}\right) T_1 + \left(s_{13}^E - \frac{s_{23}^E s_{12}^E}{s_{22}^E}\right) T_3 + \left(d_{13} - \frac{d_{32} s_{12}^E}{s_{22}^E}\right) E_3 \tag{11.a}$$

$$S_3 = \left(s_{13}^E - \frac{s_{23}^E s_{12}^E}{s_{22}^E}\right) T_1 + \left(s_{33}^E - \frac{{s_{23}^E}^2}{s_{22}^E}\right) T_3 + \left(d_{33} - \frac{d_{32} s_{23}^E}{s_{22}^E}\right) E_3 \tag{11.b}$$

$$D_3 = \left(d_{31} - \frac{d_{32} s_{12}^E}{s_{22}^E}\right) T_1 + \left(d_{33} - \frac{d_{32} s_{23}^E}{s_{22}^E}\right) T_3 + \left(\epsilon_{33}^T - \frac{{d_{32}}^2}{s_{22}^E}\right) E_3 \tag{11.c}$$

Using Eq. 11.a, T_1 is expressed as a function of S_1, T_3 and E_3, which is then inserted into Eq. 11.b and 11.c. Therefore, now, the internal energy of Eq. 9 depends on S_1^2, T_3^2, $T_3 E_3$ and E_3^2. For large aspect ratio resonators, considering T_1 close to 0, Eq. 11.a becomes:

$$S_1 = \left(s_{13}^E - \frac{s_{23}^E s_{12}^E}{s_{22}^E}\right) T_3 + \left(d_{31} - \frac{d_{32} s_{12}^E}{s_{22}^E}\right) E_3 \tag{12}$$

For small aspect ratio resonators, S_1 is close to 0. Then, we introduce a shape function $g(G)$ and the strain is written as:

$$S_1 = \left[\left(s_{13}^E - \frac{s_{23}^E s_{12}^E}{s_{22}^E}\right) T_3 + \left(d_{31} - \frac{d_{32} s_{12}^E}{s_{22}^E}\right) E_3\right] g\left(G\right) \tag{13}$$

The shape function $g(G)$ depends on the aspect ratio G and is related to the mode coupling. Its expression, mainly inspired from Kim's work,[14] is expressed as:

$$g\left(G\right) = \frac{f_a}{f_b}\frac{f_1}{f_2}\frac{1}{\sqrt{1-\Gamma^2}} \tag{14}$$

Thanks to previous observations concerning the variations of f_1 and f_2 as a function of the aspect ratio G, the shape function $g(G)$ is equal to 0 for low values of G, which is in accordance with S_1 close to 0 for low aspect ratios (plate mode). Moreover, the shape function $g(G)$ is equal to 1 for large values of G, which is in accordance with Eq. 12. Eq. 14, together with Eq. 13, is then inserted into the expression of the internal energy (Eq. 9) depending on S_1^2, T_3^2, T_3E_3 and E_3^2. All the terms are split into elastic, dielectric and coupling terms, depending respectively on T_3^2, E_3^2 and T_3E_3. Finally, the electromechanical coupling factor is written as:

$$k = \frac{d_{33} - \frac{s_{23}^E d_{32}}{s_{22}^E} + \left(g^2(G) - 1\right) \frac{\left(s_{13}^E - \frac{s_{12}^E s_{23}^E}{s_{22}^E}\right)\left(d_{31} - \frac{s_{12}^E d_{32}}{s_{22}^E}\right)}{s_{11}^E - \frac{{s_{12}^E}^2}{s_{22}^E}}}{\sqrt{\left(s_{33}^E - \frac{{s_{23}^E}^2}{s_{22}^E} + \left(g^2(G) - 1\right) \frac{\left(s_{13}^E - \frac{s_{12}^E s_{23}^E}{s_{22}^E}\right)^2}{s_{11}^E - \frac{{s_{12}^E}^2}{s_{22}^E}}\right)\left(\epsilon_{33}^T - \frac{{d_{32}}^2}{s_{22}^E} + \left(g^2(G) - 1\right) \frac{\left(d_{31} - \frac{s_{12}^E d_{32}}{s_{22}^E}\right)^2}{s_{11}^E - \frac{{s_{12}^E}^2}{s_{22}^E}}\right)}} \tag{15}$$

One can notice that, in Eq. 15, the electromechanical coupling factor k is close to the electromechanical coupling factor for a plate k_t for low values of the aspect ratio G. For large values of the aspect ratio G, Eq. 15 is close to the electromechanical coupling factor for a slender bar k'_{33}. One can notice that Eq. 15 is also valid for a 6mm or a 4mm symmetry class material and gives the same results as in Kim's work.[14]

Fig. 5 presents the variations of the electromechanical coupling factor for the PIN-PMN-PT single crystal[4] using Eq. 15. They all vary from k_t to k'_{33} as the aspect ratio G is varying from 0.1 to 10. In the case of standard PIN-PMN-PT, the electromechanical coupling coefficient is approximately constant because, in such a configuration, the mode coupling factor Γ is very low. In the case of 90° rotation PIN-PMN-PT, the electromechanical coupling coefficient is increasing from k_t to k'_{33} and the difference between these two values is related to the mode coupling factor Γ. It shows that an

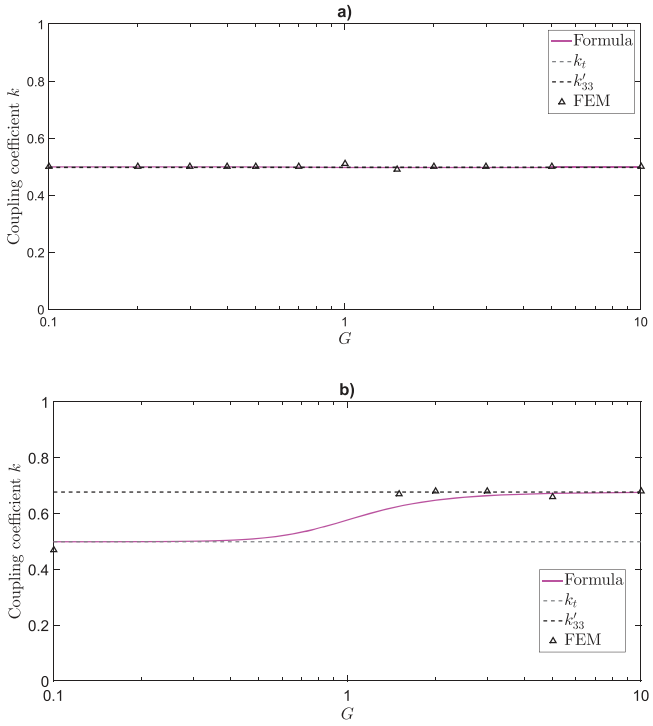


FIG. 5. Variations of the electromechanical coupling coefficient of longitudinal mode as a function of the aspect ratio G. PIN-PMN-PT single crystal (a) standard and (b) 90° rotation. (Full line: analytical model (Eq. 15), dots: FEM results.)

optimization of the material orientation has to be performed in order to maximize the electromechanical coupling factor of the device. In order to check the variations of the electromechanical coupling factor k, previous harmonic finite element calculations are used and the corresponding results for the mode under interest are reproduced with dots on Fig. 5. The numerical electromechanical coupling factor is calculated using the resonance and antiresonance frequencies.[8] The selection of the modes has been performed using the numerical displacement fields. As previously mentioned, additional numerical modes appear but only modes related to a longitudinal vibration are reproduced. They are well determined for large values of the aspect ratio G because the longitudinal mode corresponds to the first mode and is well isolated in the impedance curve. The numerical coupling factor k is determined with more difficulty for low values of the aspect ratio G because the longitudinal mode is mixed with a higher order of transversal modes. One can notice a difference between the coupling coefficients from the FEM calculation and the analytical formula when G is decreasing from large value to 1. This can be explained by the choice of the $g(G)$ function because, in spite of a reasonable justification in its determination,[14] FEM calculation shows that the variation around the value $G = 1$ is more pronounced.

IV. SUMMARY AND CONCLUSION

For piezoelectric resonator having arbitrary aspect ratio, the analytical formula relating the two longitudinal modes L-TE for a thin plate and L-WE for a slender bar is established in the general case of a mm2 piezoelectric material. Even if aspect ratios G do not correspond to an extreme geometry, electromechanical coupling factor k can be determined. Because of the anisotropic structure, an optimization on the crystal orientation is also performed in order to obtain the highest k'_{33} value, which is for example an essential criterion in ultrasonic array element design. The coupling factor Γ between the two modes studied is directly linked to the k'_{33} value. So, Γ is an important physical quantity for the electromechanical coupling optimization that could be used for future works. To develop an efficient transducer, its design has to be led in order to obtain the highest coupling factor Γ and to favor the L-WE mode. The final result of this paper also shows that, depending on the material, an aspect ratio G of 10 that can be technically difficult to reach, is not necessary to have a reasonable k'_{33}. Indeed, with an aspect ratio value of 2, the electromechanical couling factor k slightly decreases to 65% instead of 67.5% for G=10. Finally, the FEM was used throughout this work to ensure that analytical calculations were correct.

[1] Z.-G. Ye, *Handbook of advanced dielectric, piezoelectric and ferroelectric materials: synthesis, properties and applications* (Woodhead Publishing Limited, Cambridge, England, 2008).

[2] Q. Zhou, K. H. Lam, H. Zheng, W. Qiu, and K. K. Shung, "Piezoelectric single crystal ultrasonic transducers for biomedical applications," Progress in Materials Science **66**, 87–111 (2014).

[3] J. Rödel, W. Jo, K. T. P. Seifert, E.-M. Anton, T. Granzow, and D. Damjanovic, "Perspective on the development of lead-free piezoceramics," Journal of the American Ceramic Society **92**, 1153–1177 (2009).

[4] S. Zhang, G. Liu, W. Jiang, J. Luo, W. Cao, and T. R. Shrout, "Characterization of single domain $Pb(In_{0.5}Nb_{0.5})O_3$-$Pb(Mg_{1/3}Nb_{2/3})O_3$-$PbTiO_3$ crystals with monoclinic phase," Journal of Applied Physics **110**, 064108 (2011).

[5] K. Nakamura and Y. Kawamura, "Orientation dependence of electromechanical coupling factors in $KNbO_3$," IEEE Transactions on Ultrasonics, Ferroelectrics, and Frequency Control **47**, 750–755 (2000).

[6] R. Rouffaud, P. Marchet, A.-C. Hladky-Hennion, C. Bantignies, M. Pham-Thi, and F. Levassort, "Complete electroelastic set for the (YXt)-45 cut of a $KNbO_3$ single crystal," Journal of Applied Physics **116**, 194106 (2014).

[7] T. Ikeda, *Fundamentals of Piezoelectricity*, edited by O. U. Press (New York, 1996).

[8] ANSI/IEEE Standard on Piezoelectricity, "Publication and proposed revision of ANSI/IEEE standard 176-1987 "ANSI/IEEE standard on piezoelectricity"," IEEE Transactions on Ultrasonics, Ferroelectrics and Frequency Control **43**, 717 (1996).

[9] M. Kim, J. Kim, and W. Cao, "Electromechanical coupling coefficient of an ultrasonic array element," Journal of Applied Physics **99**, 074102 (2006).

[10] E. Von Giebe and E. Blechschmidt, "Experimentelle und theoretische Untersuchungen über Dehnungseigenschwingungen von Stäben und Rohren," Annalen der Physik **18**, 417–456 (I) and 457–485 (II) (1933).

[11] M. Onoe and H. Tiersten, "Resonant frequencies of finite piezoelectric ceramic vibrators with high electromechanical coupling," IEEE Transactions on Ultrasonics Engineering **10**, 32–38 (1963).

[12] O. Wilson, *Introduction to theory and design of sonar transducers* (Peninsula Publishing, Los Altos, 1988).

[13] ATILA, "Finite-Element Software Package for the analysis of 2D&3D structures based on smart materials. Version 6.0.2 User's Manual," (November 2010).

[14] M. Kim, J. Kim, and W. Cao, "Aspect ratio dependence of electromechanical coupling coefficient of piezoelectric resonators," Applied Physics Letters **87**, 132901 (2005).